Laser and Particle Beams (2010), *28*, 313–317.

doi:10.1017/S0263034610000236

Laser-driven nuclear fusion D+D in ultra-dense deuterium: MeV particles formed without ignition

SHAHRIAR BADIEI, PATRIK U. ANDERSSON, AND LEIF HOLMLID
Atmospheric Science, Department of Chemistry, University of Gothenburg, Göteborg, Sweden
(RECEIVED 18 November 2009; ACCEPTED 8 March 2010)

Abstract

The short D-D distance of 2.3 pm in the condensed material ultra-dense deuterium means that it is possible that only a small disturbance is required to give D+D fusion. This disturbance could be an intense laser pulse. The high excess kinetic energy of several hundred eV given to the deuterons by laser induced Coulomb explosions in the material increases the probability of spontaneous fusion without the need for a high plasma temperature. The temperature calculated from the normal kinetic energy of the deuterons of 630 eV from the Coulomb explosions is 7 MK, maybe a factor of 10 lower than required for ignition. We now report on experiments where several types of high-energy particles from laser impact on ultra-dense deuterium are detected by plastic scintillators. Fast particles with energy up to 2 MeV are detected at a time-of-flight as short as 60 ns, while neutrons are detected at 50 ns time-of-flight after passage through a steel plate. A strong signal peaking at 22.6 keV u^{-1} is interpreted as due to mainly T retarded by collisions with H atoms in the surrounding cloud of dense atomic hydrogen.

Keywords: ultra-dense deuterium; ultra-dense hydrogen; condensed atomic hydrogen; fusion; Coulomb explosion (CE); time-of-flight

1. INTRODUCTION

The short distance between nuclei that is required for nuclear fusion is a decisive factor for the methods of fusion energy production. In so called muon catalyzed fusion (Jackson, 1957), the average distance between the hydrogen nuclei is approximately 0.5 pm. At this distance, fusion takes place spontaneously. Other methods are however needed for fusion giving a net energy output. One important approach is inertial confinement fusion (ICF). Laser compression has been believed (Nuckolls *et al.*, 1972) to be the solution to the required high density of the target in this method, but work is still in progress after 30 years (Kodama *et al.*, 2001). Many reviews of the field and possible developments exist, with just a few recent examples cited (Ghoranneviss *et al.*, 2008; Imasaki & Li, 2008; Hora, 2007; Winterberg, 2010*b*). Here we will instead concentrate on methods to find high-density targets.

One ICF method that seems able to work at rather low densities is so-called "fast ignition" laser-induced fusion (Tabak *et al.*, 1994), with moderate laser compression and a fast igniting laser pulse. The required hydrogen density is estimated to be >300 kg dm^{-3} (Betti *et al.*, 2006). This corresponds to an average atomic density of 10^{26} cm^{-3} or an average atomic distance of 22 pm. This is a high density relative to deuterium ice, where the shortest average distance (in the D_2 molecule) is 74 pm. Liquid density clusters of deuterium give laser-induced fusion (Ditmire *et al.*, 1999; Buersgens *et al.*, 2006). It is thus possible to start fusion also in long-distance phases, and the main problem for energy generation is to assemble a dense enough initial mass so an ICF process can take place. A compression mechanism like laser compression which also gives high temperature, as well as increases the problem of maintaining a high enough density for the ICF process. Thus, alternative high-density approaches seem to be required.

One possibility is based on the solid-state enhancement of nuclear processes (Hora & Miley, 2007; Yang *et al.*, 2009), which indicates that shielding inside the bulk can give close approach of the nuclei, maybe down to 2 pm. High density clusters of hydrogen can indeed be formed inside dense metals like palladium (Lipson *et al.*, 2005). The hydrogen density is found to be on the order of 10^{24} cm^{-3}, corresponding to 100 pm distance. This is similar to the distance observed in dense hydrogen called H(1) by laser-induced

Address correspondence and reprint requests to: Leif Holmlid, Atmospheric Science, Department of Chemistry, University of Gothenburg, SE-412 96 Göteborg, Sweden. E-mail: holmlid@chem.gu.se

Coulomb explosions (Badiei & Holmlid, 2006). (The number in parentheses in H(1) indicates the Bohr angular momentum quantum number for the electrons in the material.) This condensed material has a distance of 150 pm and thus a density of 3×10^{23} cm^{-3}. A similar deuterium material D(1) also exists (Badiei *et al.*, 2009*a*, 2009*b*). The use of dense hydrogen as ICF target was proposed based on these results (Badiei & Holmlid, 2008).

Further studies of the dense hydrogen materials have shown that an even denser material exists, called ultra-dense deuterium or D(-1) (Badiei *et al.*, 2009*a*, 2009*b*). The bond distance is 2.3 pm, which is found directly from the experiments, corresponding to a density of 8×10^{28} cm^{-3}. The possible use of this material as a target material in ICF was recently discussed further (Holmlid *et al.*, 2009; Andersson & Holmlid, 2009). This material is proposed to be an inverted metal relative to D(1) (thus the -1), where the electrons and ions have exchanged their roles relative to an ordinary metal (Ashcroft, 2005; Militzer & Graham, 2006). This ultra-dense material is probably a quantum fluid (Winterberg, 2010*a*). The density of the new ultra-dense deuterium is much higher than required for ignition in "fast ignition" laser-induced fusion. By laser impact on the ultra-dense deuterium, deuterons with energy up to 1.2 keV are released (Badiei *et al.*, 2009*a*, 2009*b*). This energy may be high enough to give D+D fusion by energy transfer from fast deuterons to stationary deuterons, which are forced closer to their neighbors, initially at the distance of 2.3 pm. The selective resonant tunneling model by Li *et al.* (2004) describes the experimental cross sections for D+D fusion well. This model implies that the tunneling through the Coulomb barrier is coupled to a resonance in the nuclear well. Since the Coulomb barrier is likely to be thinner due to many-particle effects, the fusion process here may be faster than for a classical beam-target case.

To investigate the possibility of fusion with a relatively weak laser beam, we have studied the fast particles released from laser impact on ultra-dense deuterium D(-1). The experiments employ time-of-flight (TOF) particle detection with a detector (plastic scintillator), which is only sensitive to the highest kinetic energies of the ejected particles. The energy range for the particles emitted from D(-1) is 6 keV (−3 MeV), with the lower limit given by the scintillator detector. Production of such energetic particles indicates nuclear fusion of the closely located deuterons in the ultra-dense material.

2. EXPERIMENTAL

A Nd:YAG (neodymium doped yttrium aluminum garnet) pumped dye laser with a power of <100 mJ per 5 ns long pulse at 10 Hz is used at 564 nm. The laser beam is focused at the center of the ultra-high vacuum chamber by an $f = 400$ mm lens, giving an intensity of $< 5 \times 10^{11}$ W cm^{-2} at the approximately 100 μm beam waist located in the center of the chamber. Close to the center of the apparatus (Fig. 1), a K doped iron oxide catalyst sample (Meima & Menon, 2001; Holmlid, 2002; Muhler *et al.*, 1992) is used as the emitter to produce D(-1) from deuterium gas at a pressure up to 1×10^{-5} mbar. In some experiments, normal hydrogen gas is also admitted prior to D_2 gas admission to form H(1) (Badiei & Holmlid, 2006). The tantalum foil enclosing the emitter sample is cut away on the side facing the laser beam and the detector. The laser beam moves parallel to this exposed side of the emitter, with the narrow beam waist in front of its flat surface. The catalyst emitter is heated to<500 K by an alternating current through the metal foil holding the catalyst sample. The particles ejected from the emitter move through a vacuum of 2×10^{-6} mbar in the outer chamber to the detector at 112 ± 2 cm distance from the center (laser focus). In the detector, the particle beam strikes a 0.1 mm thick plastic scintillator (Nuclear Enterprises NE102A) at approximately 45° to the beam. The back side of the scintillator is covered with an aluminum layer to improve light collection. The range of protons and deuterons in the scintillator is <0.1 mm at 2 MeV, while the range of neutrons of the same energy is several meters and the detection probability of neutrons is thus very low. In the scintillator, blue photons are generated by the particle impact. These photons are observed by a photomultiplier (PMT) (EMI 6255S, rise time 8 ns, transit time 55 ns) behind a 6 mm thick blue-violet glass filter (Schott BG37, transmission 1×10^{-5} at 564 nm). The filter reduces the light from the laser to a low level. The PMT is mounted in a light tight metal container in air, outside a glass window in the vacuum wall. There is no accelerating voltage in the detector, and slow ions in the beam or secondary ions from particle impact can not be detected. The pulses from the PMT are counted by a fast TOF multichannel scaler. A photodiode close to the laser gives a fast pulse that triggers the multichannel scaler. Normally, 1500 laser shots are accumulated in each TOF spectrum. Thus, each spectrum is completed in less than 3 min. Due to the transit times in the PMT and the signal cables, the peak of the laser pulse is observed at 70–80 ns after the trigger. When the sample is moved forward against the laser beam, an increased light intensity

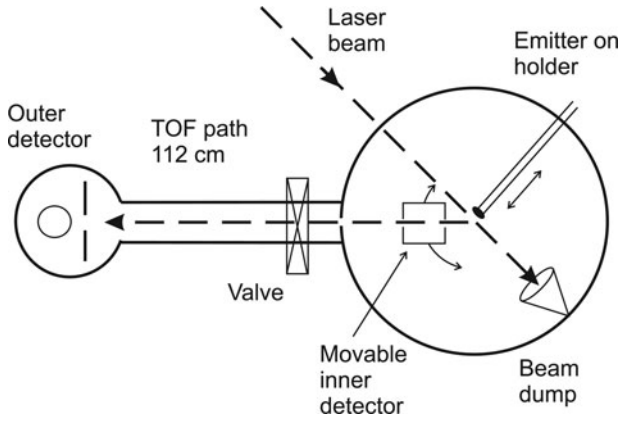

Fig. 1. Schematic drawing of the apparatus used for the laser-induced fusion studies using TOF, horizontal cut shown.

https://doi.org/10.1017/S0263034610000236 Published online by Cambridge University Press

reaches the emitter surface. This influences the signal observed by the detector and the TOF distribution changes strongly. The laser slowly depletes the D(-1) on the emitter surface, and the D(-1) layer can be restored after deuterium gas admission for a few hours. An inner detector and the thick sliding valve shown in Figure 1 at 60 cm distance from the outer detector are here used to selectively or totally block the particle beam to the scintillator detector.

3. RESULTS AND DISCUSSION

The TOF spectra shown are found after admission of deuterium gas for a few hours. It is not required that the laser impact is running for some extended period to modify the sample. On the contrary, the laser-surface interaction is either slight so that almost steady-state conditions exist (when several related spectra are compared) or immediate on a new location on the surface (when single spectra are taken). Since each spectrum corresponds to 1500 consecutive laser shots, the total time for each spectrum is slightly less than 3 min.

Typical TOF spectra are shown in Figure 2, with several settings of the PMT voltage. This gives a crude energy analysis of the PMT photon peaks, with only the largest peaks (due to the most energetic particles) observed at low PMT voltage settings. It is easily seen in the spectrum that the tail after the peak at 100 ns decreases more rapidly with PMT voltage than the peak. At the lowest PMT voltage, only a peak at 60 ns (1.8 MeV u^{-1}) is left, showing that this is the most energetic particle. The peak at 535 ns is also quite persistent, indicating high energy but longer flight time. The 1.8 MeV u^{-1} particle signal is probably due to particles with approximately one mass unit, like protons and neutrons. Thus, MeV particles are observed, which can only be formed by nuclear fusion at the low laser intensity used.

The first peak in the spectra in Figure 2, at 70 ns from zero in the plot, is mainly due to energetic quanta from the laser pulse interaction with the emitter and D(-1) material. In many cases, the gamma or X-ray photons observed penetrate into the PMT tube and give a signal already at 50 ns in the spectra, prior to any visible light from the laser that must interact with the photo cathode in the PMT.

When the laser is directed onto a fresh part of the emitter, a signal peak at 535 ns flight time is seen as in the top spectra in Figure 3. This is the same peak as seen in Figure 2, and it is only observed when both hydrogen and deuterium gas have been admitted during the day of the experiment. This peak increases in a few minutes, expanding to both shorter and longer flight times. Finally, it gives a distribution extending from 60 ns to more than 1000 ns like in Figure 2. (That the peak at 100–200 ns in Fig. 3 is slower than in Fig. 2 is probably due to too high signal prior to this peak.) The total intensity usually increases strongly simultaneously. The main peak at 535 ns has a width at half-height of 30 ns, giving particle energy of 22.6 ± 1.5 keV u^{-1}. This peak can be observed directly with an oscilloscope, and is not due to any PMT pulse pile-up or level shifting as can also be seen directly from Figure 3. The peak observed is probably due to T and ^{3}He, which have been slowed down by two collisions with protons in the cloud surrounding the emitter: only non-reactive collisions will exist with p, but nuclear reactions may take place in collisions of fast T and ^{3}He with D.

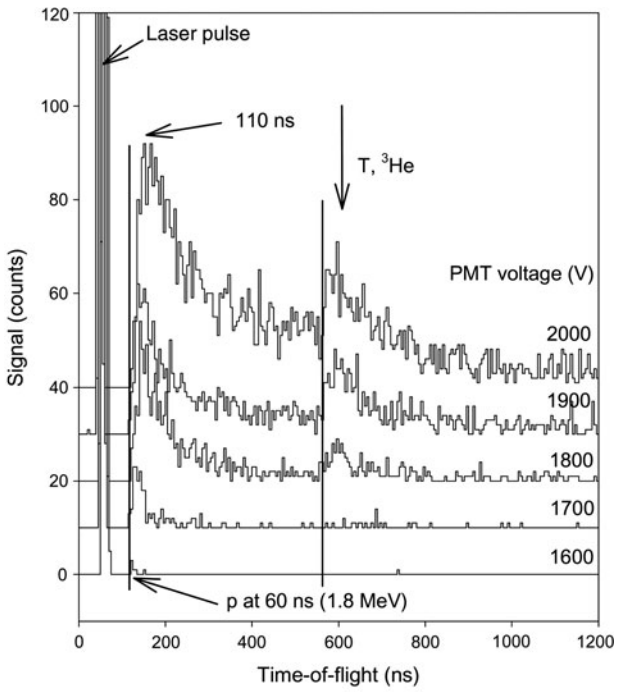

Fig. 2. Variation of TOF spectra measured with PMT voltage in the high-energy detector. Note that the peak at 60 ns with highest energy disappears last when the PMT voltage is decreased, indicating the highest photon pulses due to the 1.8 MeV kinetic energy of the protons from D+D fusion.

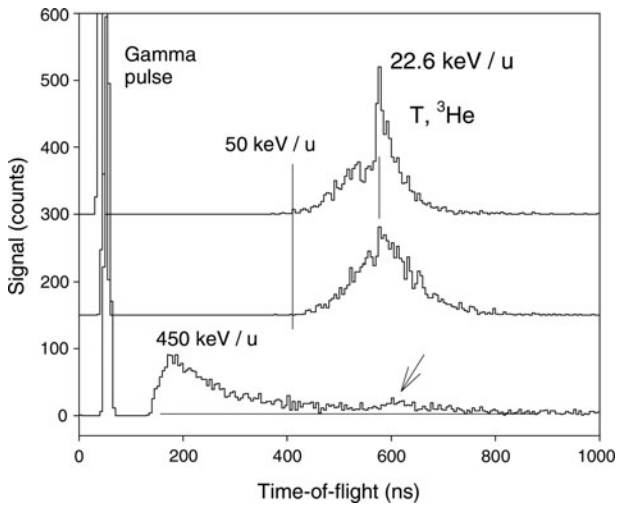

Fig. 3. TOF spectrum from the intense interaction of the D(-1) material with the laser, note the very high energy of the particles. The bottom spectrum is of the same type as in Figure 2, while the two upper spectra are from a previously unsampled spot on the D(-1) surface. The top spectrum is measured with higher TOF resolution (1 mm vertical slit in detector).

https://doi.org/10.1017/S0263034610000236 Published online by Cambridge University Press

Experiments have been done to verify that the signal in this range is due to fast charged particles and not to photons. A voltage of −8 kV to the dynode in the inner detector shown in Figure 1 provides a suitable transverse electric field to test this behavior when the two detectors are lined up. The signal is clearly influenced by the electric field. Thus, the signal is due to fast charged particles like small atomic nuclei and protons.

In Figure 4, a 1.2 mm thick steel edge in the inner detector shown in Figure 1 is rotated in small steps to block the direct flux from the laser focus to the high-energy detector. Intensity is observed at 50 ns after the laser pulse, which means particles with energy of 2.0–2.5 MeV u^{-1}. Both protons and neutrons are possible at this energy, but protons will not penetrate through the steel edge. Also faster particles are detected, possibly higher energy neutrons. The blocking quenches the gamma photon peak. (Note that the full PMT peak can not be observed at 0° since the signal is high above the discriminator level.) The signal at the laser peak decreases strongly by the blocking while the intensity at 120 ns (50 ns after the laser pulse) is unchanged; thus this fast signal is not due to any pile-up or other electronic effects. Those particles can pass through 1.2 mm stainless steel and are thus MeV neutrons.

The only other particles that may give a signal in the detector after passage through the steel edge are energetic photons (X-ray or gamma photons). However, such photons are unlikely to be delayed so that they give a peak in the TOF distribution 50 ns after the laser pulse. Thus TOF measurements provide a direct discrimination between energetic photons and neutrons, as demonstrated by Buersgens *et al.* (2006). (Their Fig. 1 shows a better resolved case than ours due to their longer flight path.) The decay time of the scintillator is 2–3 ns, so the TOF measurement is accurate. The detection takes place by neutron collisions with protons in the plastic scintillator giving electronic excitation and light emission. Further studies (unpublished) of the 50 ns peak show a quadratic signal variation with laser intensity, which is unlikely for photon production but expected for neutrons produced in pair-wise high-energy deuteron collisions. The 50 ns signal peak is related to the laser pulse in time and does not exist without the laser pulse fed into the chamber. It is possible to remove the fast TOF signal by closing the thick stainless steel plate sliding valve shown in Figure 1, which shows that the signal is formed at the laser focus. The attenuation factor for neutrons in stainless steel is close to 0.15 cm^{-1}, corresponding to an attenuation length of 7 cm. Both small-angle deflection and small energy loss in scattering events will remove the neutrons from the 50 ns peak observed by the small distant detector.

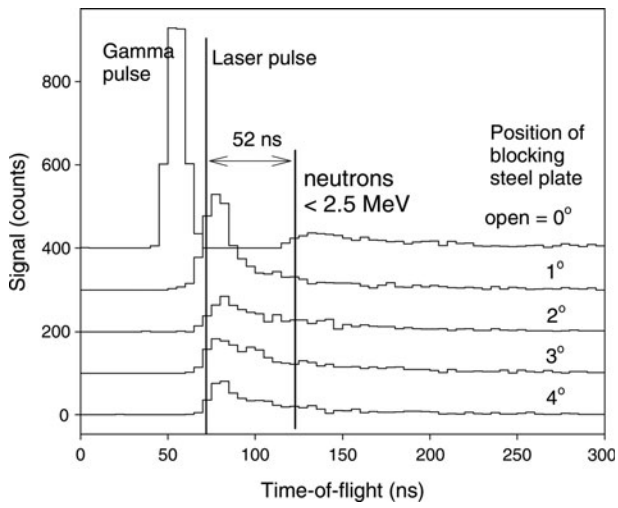

Fig. 4. Blocking of the flux to the high-energy detector by a movable steel plate. Rotation to 1° gives almost complete blocking. The full laser peak can not be observed at 0° since the signal is high above the discriminator level. All particles after the laser pulse at 70 ns are neutrons since they penetrate the steel plate. 2.45 MeV neutrons from D+D fusion are expected at 52 ns, while 14 MeV neutrons from T+D fusion are expected at 22 ns after the laser pulse.

Fast neutrons with energy of 2.5 MeV as found here are not easily detected when TOF measurements are needed. The method used by Ditmire *et al.* (1999) and Buersgens *et al.* (2006) with plastic scintillators is also used here, even if our detection efficiency is low due to the thin scintillator used. Conversion foils have been used to increase the scintillator detection efficiency by Blaich *et al.* (1992), for 1 GeV neutrons. This method has been tested here and a neutron signal at 50 ns TOF is observed also with a blocking 2 mm thick steel foil directly in front of the scintillator, however not giving an increased signal probably due to the relatively low neutron energy.

When D+D fusion takes place, the following reactions should be observed:

$$D + D \rightarrow T(1.01\,\text{MeV}) + p(3.02\,\text{MeV}), \quad (1)$$

$$D + D \rightarrow {}^{3}\text{He}(0.82\,\text{MeV}) + n(2.45\,\text{MeV}), \quad (2)$$

with 50% probability for each branch. The assignment of the neutron peak at approximately 50 ns to the neutrons emitted with 2.45 MeV (52 ns TOF calculated) is clear. The intensity of charged particles observed as the high-energy peak at 100 ns in Figure 2 and even arriving as fast as 60 ns is reasonable to identify as scattered protons initially with 3.02 MeV (47 ns TOF calculated) and other fragments. T is expected at 140 ns without scattering, and ^{3}He at 155 ns, close to the peak in Figure 2. They will however both scatter strongly within the H cloud around the emitter or even in the surface material through Coulomb forces. An analysis of the collisions of T and ^{3}He ions on their way out through the layer of D and H atoms on or outside the emitter shows that they will be slowed down to the observed energies after two sequential collisions with H atoms. In these experiments, a cloud of H(1) has been formed around the emitter by admission of hydrogen gas for 1–2 h prior to admission of D_2 gas. (Without hydrogen admission, the peak is not observed.) It is thus likely that T and ^{3}He

https://doi.org/10.1017/S0263034610000236 Published online by Cambridge University Press

scattering in the H(1) cloud gives the slower particles observed at 22.6 keV u^{-1}.

4. CONCLUSIONS

Using a plastic scintillator as detector, fast particles are observed by TOF over a 1.12 m flight distance from the interaction of a pulsed laser beam with ultra-dense deuterium. This interaction is known to give fast deuterons with energy as high as 1.2 keV. Fast particles with energy < 1.8 MeV u^{-1} are proposed to be protons from D+D fusion, with an initial energy of 3 MeV. Fast particles observed at 50 ns TOF thus with energy 2 MeV after passage through a steel edge are concluded to be neutrons, since protons cannot pass through the steel and X-rays have much shorter TOF. The intense signal peak at 22.6 keV u^{-1} is proposed to be T and ^{3}He from D+D fusion arriving with such relatively low energy after two collisions with H in the dense cloud of H(1) outside the emitter. Thus, all particles expected from D+D fusion are observed. It is assumed that the fusion cross section is increased over the beam-target value due to many-body effects at the short D-D distance of 2.3 pm.

REFERENCES

Andersson, P.U. & Holmlid, L. (2009). Ultra-dense deuterium: a possible nuclear fuel for inertial confinement fusion (ICF). *Phys. Lett. A* **373**, 3067–3070.

Ashcroft, N.W. (2005). Metallic superfluids. *J. Low Temp. Phys*. **139**, 711–726.

Badiei, S. & Holmlid, L. (2006). Experimental studies of fast fragments of H Rydberg matter. *J. Phys. B: At. Mol. Opt. Phys*. **39**, 4191–4212.

Badiei, S. & Holmlid, L. (2008). Condensed atomic hydrogen as a possible target in inertial confinement fusion (ICF). *J. Fusion Energy* **27**, 296–300.

Badiei, S., Andersson, P.U. & Holmlid, L. (2009*a*). Fusion reactions in high-density hydrogen: a fast route to small-scale fusion? *Int. J. Hydr. Energy* **34**, 487–495.

Badiei, S., Andersson, P.U. & Holmlid, L. (2009*b*). High-energy Coulomb explosions in ultra-dense deuterium: time-of-flight mass spectrometry with variable energy and flight length. *Int. J. Mass Spectrom*. **282**, 70–76.

Betti, R., Solodov, A.A., Delettrez, J.A. & Zhou, C. (2006). Gain curves for direct-drive fast ignition at densities around 300 g/cc. *Phys. Plasmas* **13**, 100703-1-4.

Blaich, Th., Elze, Th. W., Emling, H., Freiesleben, H., Grimm, K., Henning, W., Holzmann, R., Ickert, G., Keller, J.G., Klingler, H., Kneissl, W., König, R., Kulessa, R., Kratz, J.V., Lambrecht, D., Lange, J.S., Leifels, Y., Lubkiewicz, E., Proft, M., et al. (1992). A large area detector for high-energy neutrons. *Nucl. Instrum. and Meth. A* **314**, 136–154.

Buersgens, F., Madison, K.W., Symes, D.R., Hartke, R., Osterhoff, J., Grigsby, W., Dyer, G. & Ditmire, T. (2006). Angular distribution of neutrons from deuterated cluster explosions driven by femtosecond laser pulses. *Phys. Rev. E* **74**, 016403.

Ditmire, T., Zweiback, J., Yanovsky, V.P., Cowan, T.E., Hays, G. & Wharton, K.B. (1999). Nuclear fusion from explosions of femtosecond laser-heated deuterium clusters. *Nature* **398**, 489–92.

Ghoranneviss, M., Malekynia, B., Hora, H., Miley, G.H. & He, X. (2008). Inhibition factor reduces fast ignition threshold for laser fusion using nonlinear force driven block acceleration. *Laser Part. Beams* **26**, 105–11.

Holmlid, L. (2002). Conditions for forming Rydberg Matter: condensation of Rydberg states in the gas phase versus at surfaces. *J. Phys. Condens. Mat*. **14**, 13469–13479.

Holmlid, L., Hora, H., Miley, G. & Yang, X. (2009). Ultrahigh-density deuterium of Rydberg matter clusters for inertial confinement fusion targets. *Laser Part. Beams* **27**, 529–532.

Hora, H. & Miley, G.H. (2007). Maruhn–Greiner maximum of uranium fission for confirmation of low energy nuclear reactions LENR via a compound nucleus with double magic numbers. *J. Fusion Energy* **26**, 349–355.

Hora, H. (2007). New aspects for fusion energy using inertial confinement. *Laser Part. Beams* **25**, 37–45.

Imasaki, K. & Li, D. (2008). An approach of laser induced nuclear fusion. *Laser Part. Beams* **26**, 3–7.

Jackson, J.D. (1957). Catalysis of nuclear reactions between hydrogen isotopes by μ^- mesons *Phys. Rev*. **106**, 330–339.

Kodama, R., Norreys, P.A., Mima, K., Dangor, A.E., Evans, R.G., Fujita, H., Kitagawa, Y., Krushelnick, K., Miyakoshi, T., Miyanaga, N., Norimatsu, T., Rose, S.J., Shozaki, T., Shigemori, K., Sunahara, A., Tampo, M., Tanaka, K.A., Toyama, Y., Yamanaka, T. & Zepf, M. (2001). Fast heating of ultrahigh-density plasma as a step towards laser fusion ignition. *Nat*. **412**, 798–802.

Li, X.Z., Liu, B., Chen, S., Wei, Q.M. & Hora, H. (2004). Fusion cross-sections for inertial fusion energy. *Laser Part. Beams* **22**, 469–477.

Lipson, A., Heuser, B.J., Castano, C., Miley, G., Lyakhov, B. & Mitin, A. (2005). Transport and magnetic anomalies below 70 K in a hydrogen-cycled Pd foil with a thermally grown oxide. *Phys. Rev. B* **72**, 212507.

Meima, G.R. & Menon, P.G. (2001). Catalyst deactivation phenomena in styrene production. *Appl. Catal. A***212**, 239–245.

Militzer, B. & Graham, R.L. (2006). Simulations of dense atomic hydrogen in the Wigner crystal phase. *J. Phys. Chem. Solids* **67**, 2136–2143.

Muhler, M., Schlögl, R. & Ertl, G. (1992). The nature of the iron oxide-based catalyst for dehydrogenation of ethylbenzene to styrene. 2. Surface chemistry of the active phase. *J. Catal*. **138**, 413–444.

Nuckolls, J., Wood, L., Thiessen, A. & Zimmerman, G. (1972). Laser compression of matter to super-high densities: thermonuclear (CTR) applications. *Nat*. **239**, 139–42.

Tabak, M., Hammer, J., Glinsky, M.N., Kruer, W.L., Wilks, S.C. Woodworth, J., Campbell, E.M., Perry, M.D. & Mason, R.J. (1994). Ignition and high gain with ultrapowerful lasers. *Phys. Plasmas* **1**, 1626–1634.

Winterberg, F. (2010*a*). Ultradense deuterium. *J. Fusion Energe*. doi:10.1007/s10894-010-9280-4.

Winterberg, F. (2010*b*). *The release of thermonuclear energy by inertial confinement. Ways Towards Ignition*. Singapore: World Scientific.

Yang, X., Miley, G.H. & Hora, H. (2009). Condensed Matter Cluster Reactions in LENR Power Cells for a Radical New Type of Space Power Source. *AIP Conference Proc*. **1103**, 450–458.